Comparisons of Regional White Matter Diffusion in Healthy Neonates and Adults Using a 3T Head-only MR Scanner

Category: Original Research

This manuscript will be presented in 2002 RSNA and has won the RSNA Resident Research Trainee Prize, 2002.

ABSTRACT

Purpose: Normal adult and neonate brains were evaluated for regional and age-related differences in apparent diffusion coefficient (ADC) and fractional anisotropy (FA).

Materials and Methods: Normal adults (n=8, 28 ± 9 years) and neonates (n=20, 16±4 days) were imaged with a 3T head-only MR scanner using a single shot diffusion tensor imaging (DTI) sequence. Trace ADC, FA maps, directional maps of the putative directions of white matter tracts, and fiber tracking maps were obtained. Regions-of-interest (ROIs): 8 ROIs in white matter (WM) and one ROI in gray matter (GM) were predefined for the measurements of ADC and FA.

Results: Consistent with previously reported results, a global elevation of ADC ($p<0.001$) in both GM and WM and a reduction of FA ($p<0.001$) in WM are found in neonates when compared to that in adults. In addition, significant regional variations in FA and ADC are observed in both groups. While regional variations of FA and ADC in adults are less prominent, the central WM in neonates consistently exhibits a higher FA and lower ADC than cortical WM. Fiber tracking demonstrates only major WM tracts in neonates whereas fibers extended to the cortical WM in adults.

Conclusion: Although the observed regional differences in FA and ADC in neonates may be caused by structural discrepancies among ROIs, one of the most plausible explanations is the different extent of brain maturity. This finding further underscores the potential utility of using DTI for the study of brain development.

Key words: diffusion tensor imaging; echo planar imaging; white matter tracts; neonates

INTRODUCTION

Diffusion-weighted magnetic resonance imaging (DW-MRI) links MR signal intensities to the relative mobility of endogenous tissue water molecules (1). Signal alterations observed in DW images reflect, on a statistical basis, the displacement distribution of the water molecules within voxels. When the water molecules are unconstrained, the direction of motion of a given molecule is random and its position over time can be described approximately by a Gaussian distribution. When the extent of water diffuses in tissues is identical in all directions, such diffusion is normally referred to as "isotropic" diffusion or otherwise is referred to as "anisotropic" diffusion. Isotropic diffusion is normally seen in gray matter (GM) whereas anisotropic diffusion is commonly observed in white matter (WM); diffusion in the direction of the fibers is faster than that in the perpendicular direction (2, 3). Although the exact underlying biophysical mechanism(s) for the observed anisotropic behavior in WM is still under extensive scrutiny, the generally held view is that the specific organization in bundles of more or less myelinated axonal fibers restricts water molecule motion to be preferentially along the direction of the fiber (3-5). Therefore, it has been suggested that diffusion-weighted imaging sequences with a special arrangement of diffusion gradients can be employed to provide unique *in vivo* information on the structural and geometrical organization of tissues (2, 6).

Typically, diffusion gradients oriented in at least six non-collinear directions are utilized to acquire a set of images, which are used to estimate the diffusion tensor ($\underline{D}$) in each voxel (4, 5). Subsequently, quantities characterizing specific features of the diffusion process, such as the principal diffusivities (eigenvalues of $\underline{D}$), indices of diffusion anisotropy, and the principal

directions of diffusion (eigenvectors of $\underline{D}$) are computed (4, 5, 7). With these parameters, extensive research efforts have been devoted to utilize DTI for both normal subjects and patients in an attempt to yield new insights into the microstructural organization of WM that are not available with conventional MRI techniques. To this end, many investigators have demonstrated a reduction of diffusion anisotropy in normal-appearing white matter in patients with neurodegenerative disease such as MS (8-10) and AD (11), axonal injuries associated with hypoxic/ischemic conditions (12, 13) or traumatic brain injury (14), and psychiatric disorders such as schizophrenia (15, 16). These findings underscore the potential clinical utility of DTI in revealing subtle microstructural damage of WM associated with a variety of CNS diseases.

Elsewhere, DTI has also been employed for the study of brain development and consistent results have been reported in the literature. An elevation of ADC in both GM and WM and a reduction of diffusion anisotropy in WM are normally observed in the neonates as well as children when compared to adults (17-24). In addition, ADC has been shown to correlate negatively with age while FA exhibits a positive correlation, suggesting potential links between ADC, FA, and brain development (17-24). However, most of the results were obtained based on subjects who were scheduled for MR studies with clinical indications. Even though only subjects who had negative MR findings were included in data analysis, these results may not necessarily reflect normative values. In addition, results on regional measurements of diffusion anisotropy remain lacking. In this study, normal adults and healthy neonates 2-3 weeks after birth were imaged with a 3T head-only scanner in an attempt to determine the potential differences in the apparent diffusion coefficient (ADC), fractional diffusion anisotropy (FA), and the directions of major white matter tracts between the two groups. Specifically, regional

variations of FA in WM, potentially reflecting different degrees of brain maturation of WM in neonates, were investigated. We further hypothesize that the regional variations of ADC and FA in neonates may reflect the degree of brain maturity.

MATERIALS AND METHODS

A total of 20 normal neonates (10 males and 10 females; 16 ± 4 days) and eight normal adults (4 males and four females; 28 ± 9 years) were recruited for this study. Informed consent was obtained from all subjects and the experimental protocols were approved by the Institutional Review Board. Neonates were recruited from the newborn nursery of UNC Hospitals as part of an ongoing study of normal brain development. In contrast, adult subjects were recruited from the community. Neither the normal adults nor the neonates were sedated for MR imaging. Neonates were fed prior to scanning, swaddled, fitted with ear protection and had their heads fixed in a vac-fix device. A pulse oximeter was used to monitor heart rate and oxygen saturation. Most neonates slept during the scan. Since a head-only scanner was employed in this study, parents were able to sit near their babies throughout the entire imaging session.

All images were acquired on a Siemens head-only 3T scanner (Allegra, Siemens Medical System Inc., Erlangen, Germany) with a maximum gradient strength of 40 mT/m and a maximum slew rate of 400 mT/m/msec. Two main imaging sequences were employed, including a magnetization prepared rapid gradient echo (MP-RAGE) T1-weighted and a single shot echo planar (EPI) DTI sequence. For the neonate group, the imaging parameters for the DTI sequence were as follows: TR/TE/TH=4219ms/92.2ms/5mm, inplane resolution = $1.72 \times 1.72 mm^2$ with a

gap of 1mm, 12 averages, and 20 slices. Seven images were acquired for each slice, one without diffusion gradient (b=0) while the remaining six with b=1000s/mm^2 and diffusion gradients along $\{1/\sqrt{2}, 0, 1/\sqrt{2}\}$, $\{-1/\sqrt{2}, 0, 1/\sqrt{2}\}$, $\{0, 1/\sqrt{2}, 1/\sqrt{2}\}$, $\{0, 1/\sqrt{2}, -1/\sqrt{2}\}$, $\{1/\sqrt{2}, 1/\sqrt{2}, 0\}$, $\{-1/\sqrt{2}, 1/\sqrt{2}, 0\}$, separately. The imaging parameters for the MP-RAGE sequence were as follows: TR/TE/TI/TH=11.1ms/4.3ms/400ms/1mm, inplane resolution = 1.27×0.90mm^2. A total of 122 sagittal images were acquired to cover the entire brain, and the total data acquisition time was 5 min and 34 sec. All the imaging parameters remained identical for the adult group except that the TI was changed to 300msec and a total of 128 slices were acquired for the MP-RAGE sequence, resulting in a total data acquisition time of 6 min and 39 sec.

All DTI images were transferred to a PC for data analysis. Trace images were first created by averaging all six diffusion-weighted images, and subsequently ADC maps were obtained as

$$ADC=\ln(S_{b=0}/S_{b=1000})/b,$$

where $S_{b=1000}$ represents the trace DW images and $S_{b=0}$ indicates the image obtained in the absence of diffusion gradients. Subsequently, pixel-by-pixel diffusion tensor was represented by a 3×3 matrix $\underline{D}$. Analytical expressions were then obtained for the three principle diffusivities of $\underline{D}$, λ_1, λ_2 and λ_3, by solving the characteristic equation of $\underline{D}$. Additionally, the eigenvectors of $\underline{D}$ were also obtained. Subsequently, fractional diffusion anisotropy (FA) was calculated as:

$$FA=\sqrt{3[(\lambda 1-<\lambda>)^2+(\lambda 2-<\lambda>)^2+(\lambda 3-<\lambda>)^2]}\,/\sqrt{2(\lambda 1^2+\lambda 2^2+\lambda 3^2)}$$

where $< l >= (l1 + l2 + l3)/3$. Since FA measures the fraction of the "magnitudes" of $\underline{D}$ that can be ascribed to anisotropic diffusion, it varies between 0 (isotropic diffusion) and 1 (infinite anisotropy). Furthermore, the putative direction of a WM tract was defined as the eigenvector corresponding to the largest eigenvalue so that a pixel-by-pixel map of fiber directions could be obtained. In order to focus only on major white matter tracts for the fiber directional maps, an FA threshold of 0.5 and 0.3 was employed for the adult and neonate groups, respectively. Only pixels with an FA greater than the predefined threshold value were used for the calculation of the eigenvectors.

Fiber tracking

The principle diffusive direction, i.e. the eigenvector associated with the largest eigenvalue, of the local tensor indicates local orientation of fiber tracts. Tracing these local directions through white matter between user-defined source and target regions allows the reconstruction of three-dimensional trajectories following major axonal tracts. Different techniques mostly based on path finding in three-dimensional vector fields have been developed (see (25) for a most recent introduction). A fiber tracking method originally developed by Mori et al (26, 27) was modified to include volumes of interest of arbitrary shape as source and target regions for trajectories and was used in our study. Volumes of interest of the splenium and genu of the corpus callosum were first defined using the FA images and a multiplanar visualization tool. The target was defined as the whole brain cortex to search for all possible trajectories originating from the two source locations. DTI images obtained from 3 neonates and one adult were employed for fiber tracking so as to explore the potential discrepancies between neonates and adults.

Region-of-interest (ROI) analysis

An ROI approach was employed for measuring both FA and ADC from both adults and neonates. In each subject, nine ROIs were predefined on a single transverse section through the level of the basal ganglia. Eight ROIs were placed in white matter, including the anterior and posterior limbs of the internal capsule, the genu and splenium of the corpus callosum, left and right occipital and frontal WM adjacent to the cortical gray matter. Results obtained from the anterior and posterior limbs of the internal capsule, the left and right occipital white matter, the left and right frontal WM were averaged separately for subsequent data analysis. These white matter structures were chosen because they exhibited visible anisotropy and were easily identified on diffusion-tensor images. The remaining ROI was placed in the cortical gray matter. Special care was taken to exclude contributions from cerebrospinal fluid (CSF) for the choice of ROIs by comparing FA and ADC maps with the b=0 images.

Statistical Analysis

Student's t-test was employed for the comparison of experimentally measured FA and ADC between adults and neonates. In addition, a single factor ANVOA correcting for multiple comparisons (Tukey's multiple comparison test) was employed to determine whether or not regional differences in both FA and ADC were significant. A p-value < 0.05 was considered significant at a 95% confidence level.

RESULTS

We were able to obtain high quality DW images without apparent motion artifact on 13 of the 20 neonates (8 males, 5 females). Representative sagittal as well as the reconstructed transverse MP-RAGE images from one neonate (Fig. 1a and b) and one adult (Fig. 1c and d) are shown,. While the total data acquisition time for the MP-RAGE was shorter in the neonate group than that in the adult group, the image quality is adequate. Clearly, the gray/white contrast in the images obtained from the adult group is superior to that in the neonate group. In addition, gray/white contrast is reversed between neonates and adults.

Typical b=0 images (Fig. 2a and d), ADC (Fig. 2b and e), and FA maps (Fig. 2c and f) are shown from one neonate (Fig. 2a-c) and one adult (Fig. 2d-e) in Fig. 2, respectively. As anticipated, the gray/white contrast is reversed in the T2-weigthed images between the neonate and the adult groups. In addition, while it is difficult to discern gray and white matter on ADC images for both the adult and neonate groups, an obvious difference in FA between the gray matter and white matter is seen for both groups; white matter exhibits a higher FA than that in gray matter. However, only the major white matter tracts exhibit a higher FA value in the neonate group as opposed to the adult group where the whole brain white matter demonstrates a higher FA value when compared to that in gray matter.

Quantitative measurements of ADC from both the adult and neonate groups are shown in Fig. 3a. ADC values in the neonate group are significantly higher ($p<0.001$) than that in the adult group for all ROI assessed. For the neonate group, significantly higher ADC values are observed in

both cortical white matter as well as gray matter regions when compared to central white matter. Statistical comparisons of different ROIs are summarized in Table 1. In contrast, ADC in the adults is more homogeneous across WM regions with small, but statistically significant differences (Table 1). Finally, when the ADC ratios of neonates to adults are compared (Fig.3b), the frontal white matter exhibiting the highest ratio (2.05) followed by cortical GM, occipital WM, the genu of corpus callosum, the internal capsule, and the splenium of corpus callosum.

Fig. 4a shows the FA values for both the adult and neonate groups. FA is significantly higher in adults compared to neonates for all of the regions assessed ($P<0.001$). In the neonate group, FA is higher in central white matter compared to cortical white matter and gray matter. Results of regional comparisons of FA are given in Table 1. In contrast, the extent to which FA varies among WM ROIs in adults is less remarkable than that observed in neonates, although statistical differences remain (Table 1) between some ROIs. The FA ratios between neonates and adults are shown in Fig. 4b. Similar to the characteristics of ADC ratios between neonates and adults, a substantial regional variation in the FA ratios is observed. However, except for GM, the order of the magnitude of the ratios is exactly opposite to that observed in ADC ratios, the splenium of corpus callosum has the highest ratio followed by the internal capsule, the genu of corpus callosum, occipital WM, and frontal WM.

The primary eigenvectors, reflecting the putative directions of the white matter fibers are shown in Fig. 5 for one neonate (Fig. 5a) and one adult (Fig. 5b). While only the major white matter tracts are seen in the neonate group, no apparent differences are observed between the two groups.

Finally, representative results obtained from fiber tracking are shown in Fig. 6 from one neonate (upper row) and one adult (lower row). Fibers were tracked from the splenium and genu to the brain surface, using the same computer program parameters. The resulting traces are overlaid with transversal and mid-sagittal contour plots of the DTI b=0 images to augment three-dimensional visualization. Although preliminary, the results suggest that major white matter tracts can be fully traced to cortical areas in the adult group but are limited to major interior tracts in the neonates.

DISCUSSION

This study indicates that it is possible to obtain high quality diffusion tensor imaging data in unsedated newborns using a fast DTI sequence on a 3T scanner. We found that neonates had significantly higher white matter ADC ($p<0.001$) and significantly lower white matter FA ($p<0.001$) compared to adults. These findings are consistent with previous reports (13, 17, 18, 21, 22, 28). We report for the first time that there is a significant difference in FA and ADC in central white matter compared to cortical white matter in neonates. Quantitative measurements in our study reveal ADC (10^{-11} mm^2/sec) ranging between 153.9 ± 10.3 (occipital white matter) and 115.0 ± 20.3 (splenium of corpus callosum) among white matter ROIs and 134.5 ± 22.9 for gray matter whereas the FA is between 0.20 ± 0.07 (frontal white matter) and 0.63 ± 0.06 (splenium of corpus callosum) among white matter ROIs and 0.10 ± 0.03 in gray matter for the neonate group. In contrast, in the adult group, the ADC (10^{-11} mm^2/sec) ranges between 71.5 ± 4.2 (internal capsule) and 88.7 ± 6.7 (occipital white matter) across white matter and $112.6 \pm$

10.7 in gray matter while the FA lies between 0.58 ± 0.06 (occipital white matter) and 0.78 ± 0.02 (genu of corpus callosum) among white matter and 0.16 ± 0.03 for gray matter. These results are comparable with several studies reported in the literature (12, 17, 29). Specifically, Engelbrecht et al. (17) imaged 44 children ranging from 7 days to 7.5 years with DWI. Of the 44 subjects studied, 5 subjects were about 1 month old, similar to the age group in our studies. With this five subjects, the reported ADC (10^{-11} mm^2/sec) ranges between 104 – 164, in good agreement with the ranges of ADC observed in our studies. In addition, similar to our findings, the occipital white matter exhibited the highest ADC and the internal capsule had the lowest ADC among the white matter ROIs evaluated. Nevertheless, ADC values obtained from the occipital white matter and the internal capsule appear to be higher in their studies when compared to that obtained in our studies, most likely reflecting the differences in the ages of subjects between the two studies.

It has been suggested that the increase of brain water content in neonates may account for the observed elevation of ADC in neonates as compared to adults. Neil et al (22) imaged 22 newborns 36 hrs after birth. Both ADC and quantitative diffusion anisotropy were measured from all subjects. They reported that a correlation existed between ADC and the gestational age, suggesting the potential role of brain water for the observed elevated ADC in neonates when compared to adults. However, no clear relationship was observed when quantitative diffusion anisotropy was correlated to the gestational age (22). Their findings are perhaps not surprising given the fact that ADC provides an assessment of the overall water mobility. In the neonate brain where brain water content is higher than that in adults, leading to, potentially, less water restriction by either membranes or other physiological barriers and thus resulting in a higher

ADC. In contrast, diffusion anisotropy is more directly associated with the extent of white matter development and thus should not be affected by the extent of brain water content. Therefore, a potential correlation between age and the extent of white matter anisotropy may be explained by this mechanism.

Indeed, a direct correlation between white matter anisotropy and age is reported by many investigators (17, 20, 23, 29, 30). The general findings are that diffusion anisotropy in white matter increases from infancy to adulthood and subsequently decreases with aging (29, 30), further confirming the potential utility of DTI for the investigation of brain development. However, the exact relationship between the two parameters appears to vary among different reported results. With subjects between 5-18 years old, Schmithorst et al (23) converted all the acquired images onto the Talairarch space. A pixel-by-pixel analysis was performed to determine regions where FA changes were correlated with ages. They concluded that a linear relationship between FA and age existed. In contrast, Mukherjee et al. (20) demonstrate an exponential increase of diffusion anisotropy with age for subjects between 1 day to 11 years old in both the posterior limb of the internal capsule and thalamus, although a linear relationship was also observed at the lentiform nucleus. Furthermore, results reported by Engelbrecht et al. based on subjects between 7 days and 7.5 years old appear to be best characterized by a function expressed as A(1-exp(-age)) where A is a constant. While the differences in ages for the subjects studied may account for the observed discrepancies in the relationship between diffusion anisotropy and ages, the most likely explanation is the potential regional variations in the measurements of diffusion anisotropy. As shown in Figs. 3 and 4, substantial and statistically significant regional variations exist in the measurements of ADC and FA for both the adult and

neonate groups. Therefore, in addition to taking into account the potential age dependence of FA and ADC, regional variations of both parameters should be considered when comparing results obtained from different studies.

Relationship between regional variations of FA and ADC and brain development in neonates

The observed regional variations in FA and ADC require additional discussion. While regional differences are observed between the adult and neonate groups, they are more substantial in neonates. Therefore, the subsequent discussion will focus only on the regional variations of ADC and FA observed in neonates. Most of the studies to date have emphasized the potential relationship between diffusion anisotropy and age, with relatively little attention regarding the potential implications of regional variations of FA and ADC in the same age population. Specifically, as mentioned previously, several lines of evidence have suggested that measurements of diffusion anisotropy may reflect brain maturity. Therefore, we hypothesize that the observed regional variations in FA and ADC for the neonate group could reflect the regional extent of brain maturity 2 weeks after birth. As shown in Fig. 4a, among the white matter ROIs evaluated, the splenium of corpus callosum exhibits the highest FA, followed by the genu of corpus callosum, the internal capsule, occipital white matter, and frontal white matter. In addition, when FA of each ROI in the neonate group is normalized to the corresponding region of the adult group (Fig. 4b), the FA at the splenium of corpus callosum is most comparable, while the frontal white matter is less similar to that obtained from the adult group. In other words, if one assumes that the measurements of FA reflect the degree of brain maturity, the splenium of corpus callosum will be the most advanced and the frontal white matter is the least developed region 2 weeks after birth. In contrast, although it is immediately obvious that the

ADC values of the central white matter are higher than those of the cortical white matter, the order of magnitude of ADC values at different ROI is not apparent. However, when the ADC ratios of neonates to adults are examined, the order of the magnitude is exactly opposite to that observed with FA ratios; the frontal white matter exhibits the highest ratio and the splenium of corpus callosum has the lowest ratio. This is of interest, since it is well known that brain water is expected to decrease as the brain develops and this has been suggested as one of the primary factors contributing to the elevation of ADC in neonates (22). The observed order of ADC ratios would imply that the frontal white matter is less developed while the splenium of corpus callosum is the most advanced in the brain development, identical conclusions to those based on the FA ratios.

The regional variations of FA and ADC found in our study are in good agreement with the known temporal order of brain myelination. As summarized by Volpe (31), the pattern of brain myelination starts from proximal to distal pathways, from sensory to motor, from projection to associative pathways. Furthermore, Volpe (31) also indicated the occipital lobe completes the myelination process prior to frontal lobe. In addition, Knaap et al (32) studied the evolution of cerebral gyration and sulcation in preterm and term neonates in an attempt to determine brain development. Both T1-weighted and T2-weighted images were employed for their studies. They reported that at birth the gyral development was most advanced in the central sulcus and the medial occipital lobe, while most immature at the frontal and temporal regions. Therefore, these findings support our hypothesis that the regional discrepancies of FA and ADC may be indicative of different brain maturity levels in different brain regions. More studies, including

longitudinally following the same subjects will be needed to further assess the implications of regional variations of FA and ADC observed in the neonate group.

Our study has three major advantages. First, unlike most of the studies where images obtained from subjects who were scheduled for MR imaging due to clinical indications were analyzed, normal neonates were recruited for our studies. Therefore, our results should directly reflect the normative ADC and FA values for the age range included in our studies. Second, none of the neonates were sedated, minimizing the potential confounding factors associated with sedation in the measurements of ADC and FA. Finally, a 3T head-only scanner was employed. With the improved signal-to-noise ratio, it was possible to shorten the total data acquisition time while maintaining an adequate signal-to-noise ratio, minimizing motion artifacts. Conversely, our study has two technical limitations. First, in order to minimize diffusion gradient induced motion artifacts, a single shot EPI sequence was employed in our studies, resulting in limited spatial resolution, particularly for the neonate group. This limited spatial resolution is likely to induce partial volume effects and can potentially confound the ROI measurements of FA and ADC in our studies. Second, the results of fiber tracking are preliminary and the accuracy of this method has yet to be established. Nevertheless, our preliminary results suggest different patterns in fiber-tracked tracts between neonates and adults. More studies will be needed to further determine the clinical utility of fiber tracking.

In summary, we have observed substantial regional variations of FA and ADC in neonates and demonstrated statistically significant differences in FA and ADC between adults and neonates, using DTI. More importantly, when regional ADC and FA measurements from neonates are

normalized to those of the corresponding region from adults, the order of the magnitude of the ratios exhibits a pattern that is consistent with the temporal order of brain myelination; the splenium of corpus callosum has the highest FA ratio but the lowest ADC ratio, whereas the frontal white matter demonstrates the lowest FA ratio but the highest ADC ratio. These findings suggest that the splenium of corpus callosum is in the most advanced stage of brain development while the frontal white matter is the least developed at 2-3 weeks after birth, compared to the remaining ROIs assessed. The ability to non-invasively assess the degree of brain development in neonates should offer an important means to study white matter development in children at risk for neurodevelopmental and neuropsychiatric disorders as well as, potentially, to monitor response to therapeutic interventions.

REFERENCES

1. Mintorovitch J, Cohen Y, Asgari HS, et al. Diffusion-weighted MR imaging of the brain: value of differentiating between extraaxial cysts and epidermoid tumors. Acta Neurochirurgica - Supplementum 1990;51:207-209.
2. Basser PJ. Inferring microstructural features and the physiological state of tissues from diffusion-weighted images. NMR in Biomedicine 1995;8:333-344.
3. Barkovich AJ. Concepts of myelin and myelination in neuroradiology. Ajnr: American Journal of Neuroradiology 2000;21:1099-1109.
4. Basser PJ and Pierpaoli C. A simplified method to measure the diffusion tensor from seven MR images. Magnetic Resonance in Medicine 1998;39:928-934.
5. Shrager RI and Basser PJ. Anisotropically weighted MRI. Magnetic Resonance in Medicine 1998;40:160-165.
6. Le Bihan D. Molecular diffusion, tissue microdynamics and microstructure. NMR in Biomedicine 1995;8:375-386.
7. Basser PJ and Pierpaoli C. Microstructural and physiological features of tissues elucidated by quantitative-diffusion-tensor MRI. Journal of Magnetic Resonance Series B 1996;111:209-219.
8. Ciccarelli O, Werring DJ, Wheeler-Kingshott CA, et al. Investigation of MS normal-appearing brain using diffusion tensor MRI with clinical correlations. Neurology 2001;56:926-933.
9. Griffin CM, Chard DT, Ciccarelli O, et al. Diffusion tensor imaging in early relapsing-remitting multiple sclerosis. Multiple Sclerosis 2001;7:290-297.

10. Mainero C, De Stefano N, Iannucci G, et al. Correlates of MS disability assessed in vivo using aggregates of MR quantities. Neurology 2001;56:1331-1334.

11. Rose SE, Chen F, Chalk JB, et al. Loss of connectivity in Alzheimer's disease: an evaluation of white matter tract integrity with colour coded MR diffusion tensor imaging. Journal of Neurology, Neurosurgery & Psychiatry 2000;69:528-530.

12. Wolf RL, Zimmerman RA, Clancy R, Haselgrove JH. Quantitative apparent diffusion coefficient measurements in term neonates for early detection of hypoxic-ischemic brain injury: initial experience. Radiology 2001;218:825-833.

13. McKinstry RC, Miller JH, Snyder AZ, et al. A prospective, longitudinal diffusion tensor imaging study of brain injury in newborns. Neurology 2002;59:824-833.

14. Arfanakis K, Haughton VM, Carew JD, Rogers BP, Dempsey RJ, Meyerand ME. Diffusion tensor MR imaging in diffuse axonal injury. Ajnr: American Journal of Neuroradiology 2002;23:794-802.

15. Taber KH, Pierpaoli C, Rose SE, et al. The future for diffusion tensor imaging in neuropsychiatry. Journal of Neuropsychiatry & Clinical Neurosciences 2002;14:1-5.

16. Foong J, Symms MR, Barker GJ, Maier M, Miller DH, Ron MA. Investigating regional white matter in schizophrenia using diffusion tensor imaging. NeuroReport 2002;13:333-336.

17. Engelbrecht V, Scherer A, Rassek M, Witsack HJ, Modder U. Diffusion-weighted MR imaging in the brain in children: findings in the normal brain and in the brain with white matter diseases. Radiology 2002;222:410-418.

18. Martin KM, Mustafa MH, Wilkinson ID, et al. Study of pediatric brain development using magnetic resonance imaging of anisotropic diffusion. Magnetic Resonance in Medicine 2002;48:394-398.

19. Mori S, Itoh R, Zhang J, et al. Diffusion tensor imaging of the developing mouse brain. Magnetic Resonance in Medicine 2001;46:18-23.

20. Mukherjee P, Miller JH, Shimony JS, et al. Normal brain maturation during childhood: developmental trends characterized with diffusion-tensor MR imaging. Radiology 2001;221:349-358.

21. Mukherjee P, Miller JH, Shimony JS, et al. Diffusion-tensor MR imaging of gray and white matter development during normal human brain maturation. AJNR Am J Neuroradiol 2002;23:1445-1456.

22. Neil J, Shiran S, McKinstry R, et al. Normal brain in human newborns: apparent diffusion coefficient and diffusion anisotropy measured by using diffusion tensor MR imaging. Radiology 1998;209:57-66.

23. Schmithorst VJ, Wilke M, Dardzinski BJ, Holland SK. Correlation of white matter diffusivity and anisotropy with age during childhood and adolescence: a cross-sectional diffusion-tensor MR imaging study. Radiology 2002;222:212-218.

24. Huppi PS, Maier SE, Peled S, et al. Microstructural development of human newborn cerebral white matter assessed in vivo by diffusion tensor magnetic resonance imaging. Pediatric Research 1998;44:584-590.

25. Basser PJ, Pajevic S, Pierpaoli C, Duda J, Aldroubi A. In vivo fiber tractography using DT-MRI data. Magnetic Resonance in Medicine 2000;44:625-632.

26. Melhem ER, Mori S, Mukundan G, Kraut MA, Pomper MG, van Zijl PC. Diffusion tensor MR imaging of the brain and white matter tractography. AJR. American Journal of Roentgenology 2002;178:3-16.

27. Mori S, Kaufmann WE, Davatzikos C, et al. Imaging cortical association tracts in the human brain using diffusion-tensor-based axonal tracking. Magnetic Resonance in Medicine 2002;47:215-223.

28. Boujraf S, Luypaert R, Shabana W, De Meirleir L, Sourbron S, Osteaux M. Study of pediatric brain development using magnetic resonance imaging of anisotropic diffusion. Magnetic Resonance Imaging 2002;20:327-336.

29. Pfefferbaum A, Sullivan EV, Hedehus M, Lim KO, Adalsteinsson E, Moseley M. Age-related decline in brain white matter anisotropy measured with spatially corrected echo-planar diffusion tensor imaging. Magnetic Resonance in Medicine 2000;44:259-268.

30. Abe O, Aoki S, Hayashi N, et al. Normal aging in the central nervous system: quantitative MR diffusion-tensor analysis. Neurobiology of Aging 2002;23:433-441.

31. Volpe JJ. Neurology of the newborn. Philadelphia: WB Saunders 1995.

32. van der Knaap MS, van Wezel-Meijler G, Barth PG, Barkhof F, Ader HJ, Valk J. Normal gyration and sulcation in preterm and term neonates: appearance on MR images. Radiology 1996;200:389-396.

Table 1: Statistical comparisons of regional ADC and FA in the adult and neonate groups, Separately

	Apparent Diffusion Coefficients						Fractional Anisotropy					
Adults / **Neonates**	Splenium	Genu	Internal Capsule	Occipital	Frontal	GM	Splenium	Genu	Internal Capsule	Occipital	Frontal	GM
Splenium		NS	P<.01	P<.05	NS	NS		NS	P<.05	P<.001	P<.001	P<.001
Genu	NS		NS	P<.001	NS	NS	P<.001		P<.05	P<.001	P<.001	P<.001
Internal Capsule	NS	NS		P<.001	NS	NS	P<.001	NS		P<.001	P<.05	P<.001
Occipital	P<.001	P<.001	P<.001		P<.001	P<.001	P<.001	P<.001	P<.001		NS	P<.001
Frontal	P<.001	P<.001	P<.001	NS		NS	P<.001	P<.001	P<.001	NS		P<.001
GM	P<.05	NS	P<.001	P<.05	NS		P<.001	P<.001	P<.001	P<.001	P<.05	

FIGURE CAPTIONS

Fig. 1 MP-RAGE T1-weighted images obtained from both a neonate (a and b) and an adult (c and d) are shown for comparison. It is evident that the gray and white matter contrast in the images obtained from the adult is reversed and superior to that obtained from the neonate. In addition, the signal-to-noise is also higher in images obtained from the adult when compared to the neonate.

Fig. 2 Comparisons of T2-weighted images (a and d), FA maps (b and e), and ADC maps (c and f) between the neonate (upper row) and the adult (lower row) are shown.

Fig. 3 Regional measurements of ADC in both adults and neonates are shown in a, respectively. The standard deviation indicates intersubject variability. In addition, the regional ADC ratios between neonates to adults are also given in b.

Fig. 4 Regional measurements of FA in both adults and neonates are shown in a, respectively, whereas regional FA ratios between neonates to adults are given in b.

Fig. 5 Putative direction maps of the major white matter tracts are shown from one neonate and one adult, respectively. The color bars indicate the angles of the major white matter tracts in degrees with the zero degree corresponding to the positive x-axis.

Fig. 6 Comparison of fiber tracking results obtained from a neonate (upper row) and an adult (lower row) subject. Fibers were tracked from the splenium and genu of the corpus callosum to

the brain surface. The images illustrate top views (left), left views (middle) and top-oblique views (right). The resulting traces are overlaid with transversal and mid-sagittal contour plots of the DTI b=0 images.

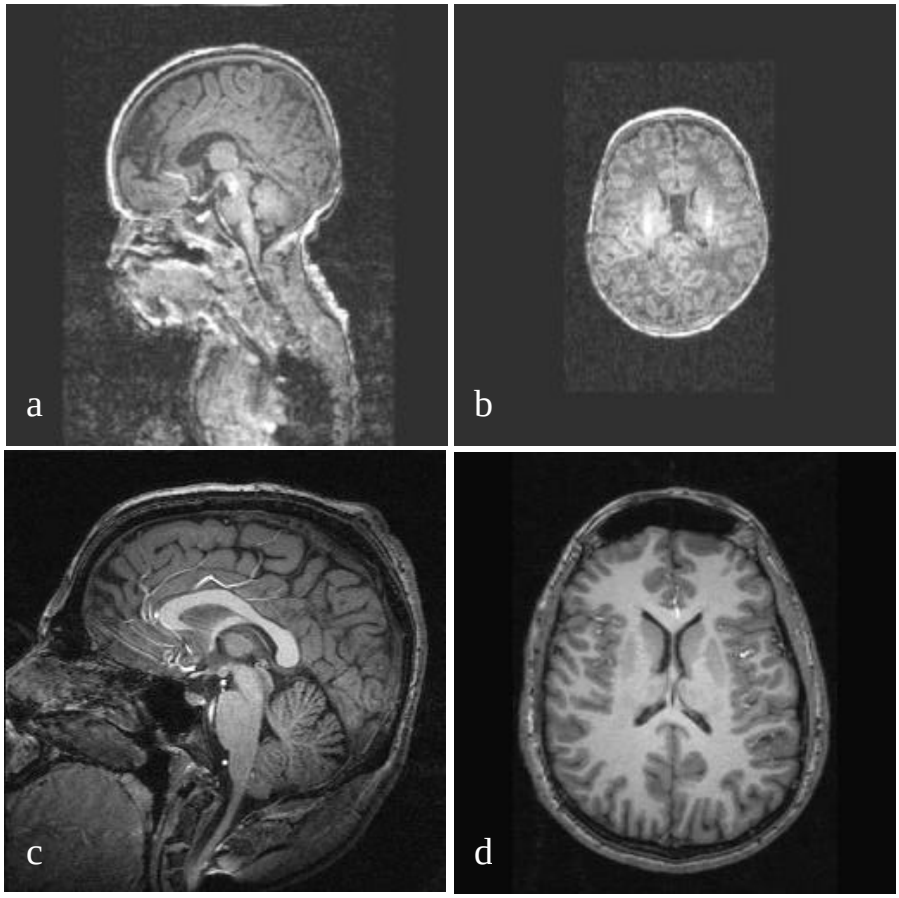

Fig. 1 MP-RAGE T1-weighted images obtained from both a neonate (a and b) and an adult (c and d) are shown for comparison. It is evident that the gray and white matter contrast in the images obtained from the adult is superior to that obtained from the neonate. In addition, the signal-to-noise is also higher in images obtained from the adult when compared to the neonate.

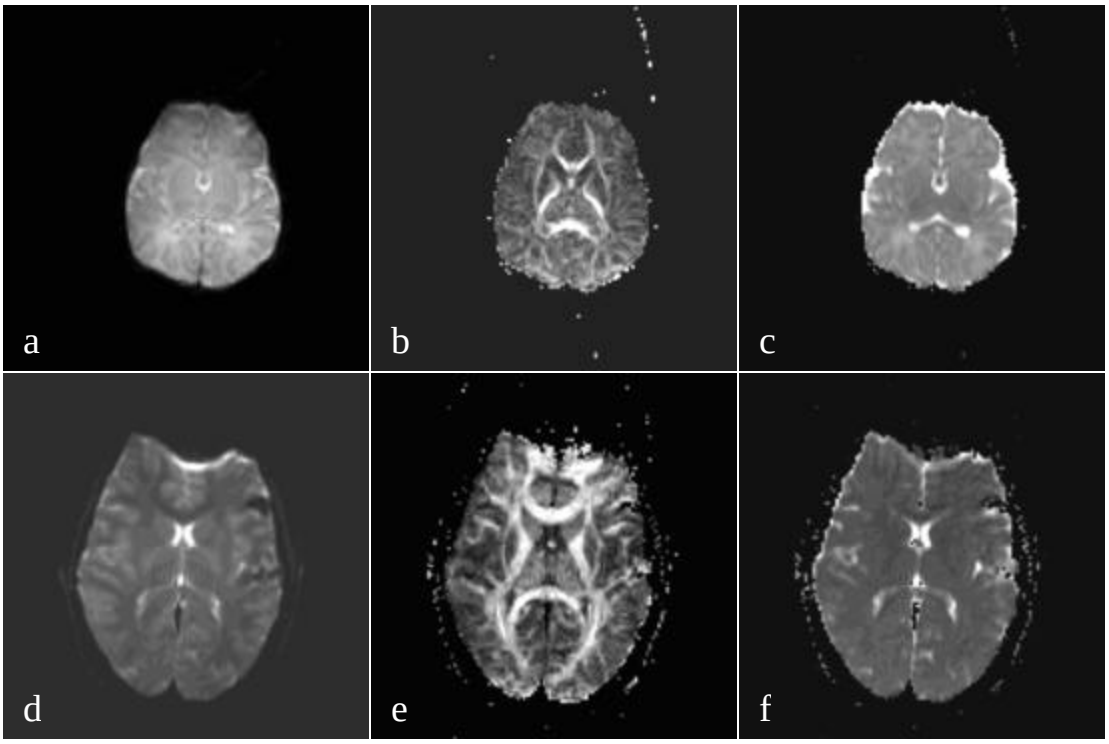

Fig. 2 Comparisons of T2-weighted images (a and d), FA maps (b and e), and ADC maps (c and f) between the neonate (upper row) and the adult (lower row) are shown.

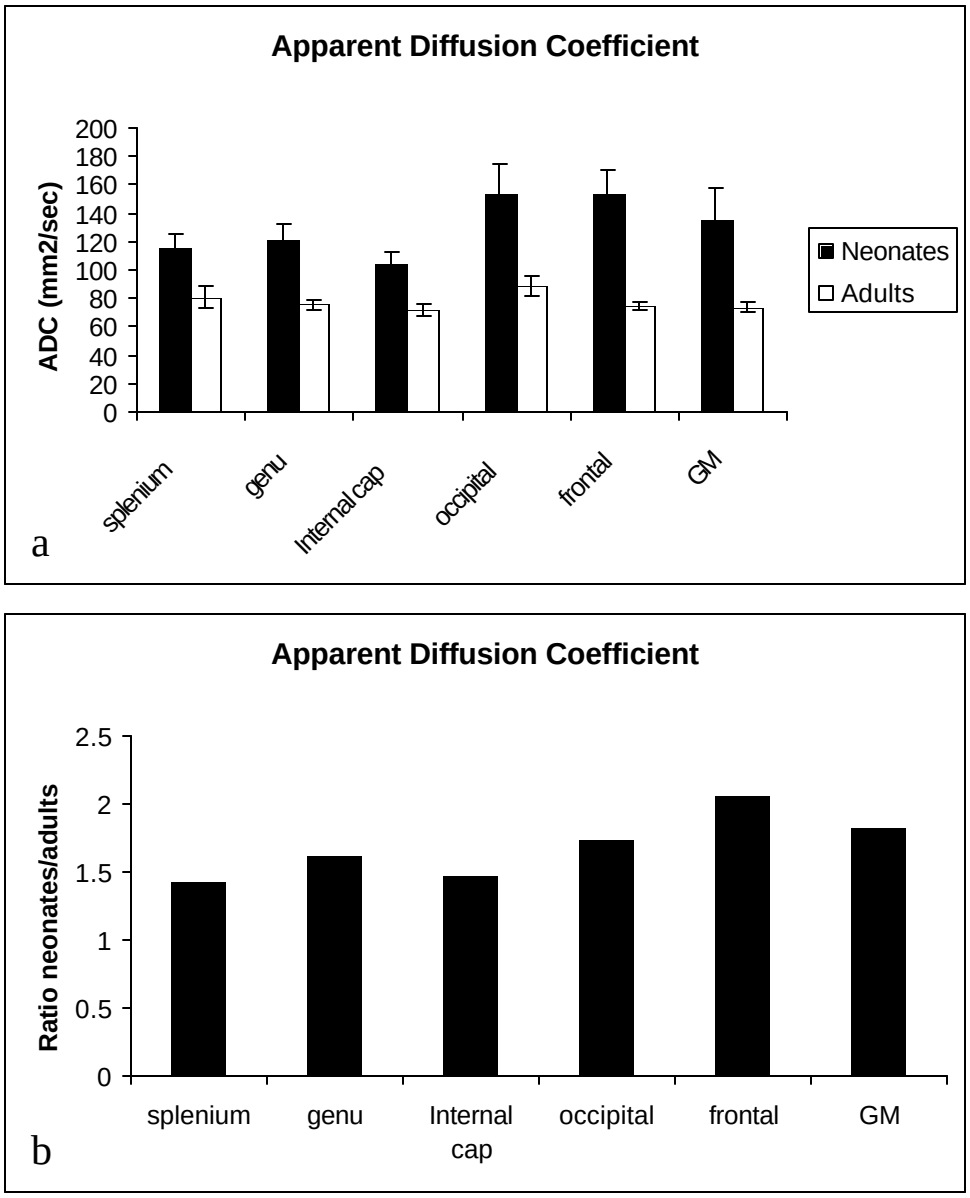

Fig. 3 Regional measurements of ADC in both adults and neonates are shown in a, respectively. The standard deviation indicates intersubject variability. In addition, the regional ADC ratios between neonates to adults are also given in b.

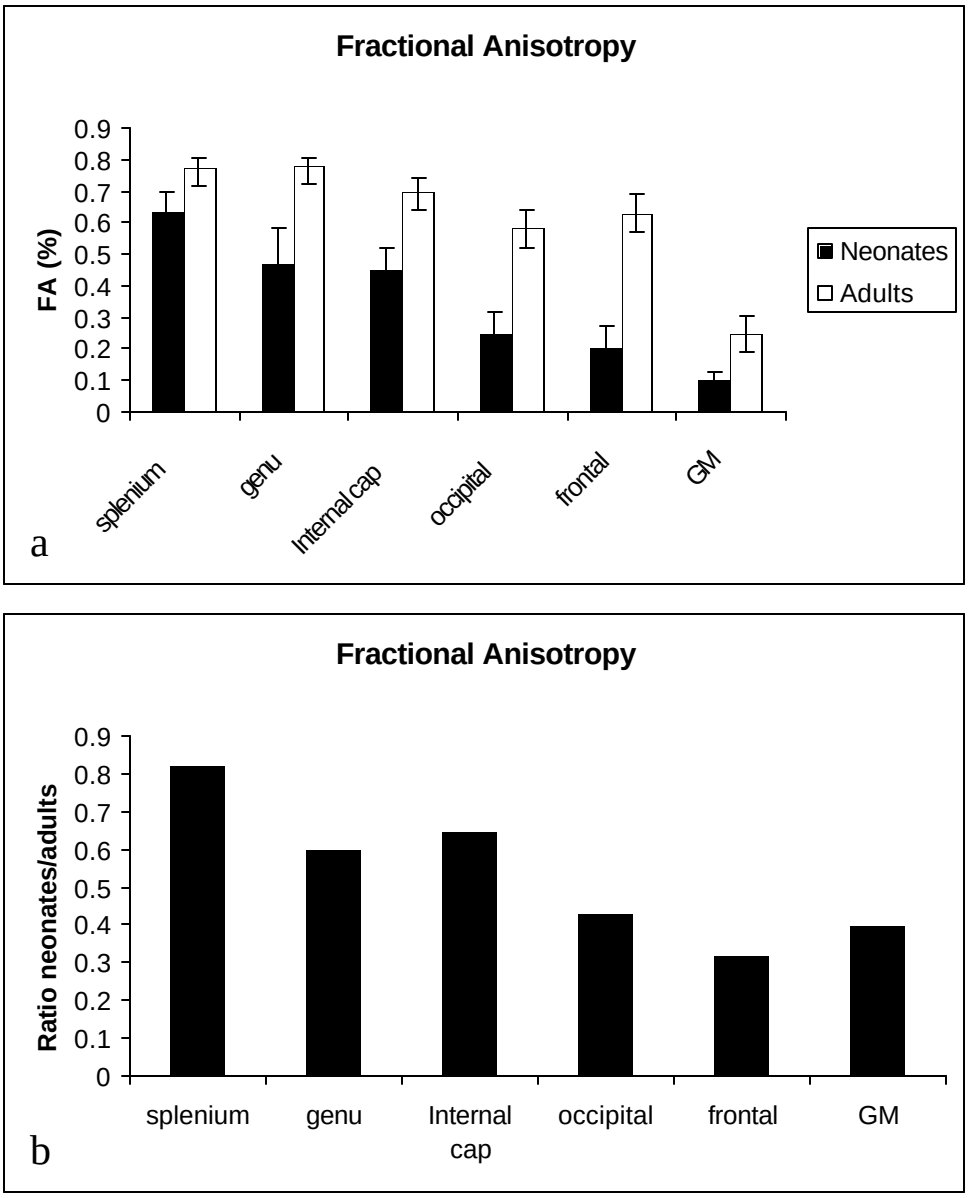

Fig. 4 Regional measurements of FA in both adults and neonates are shown in a, respectively, whereas regional FA ratios between neonates to adults are given in b.

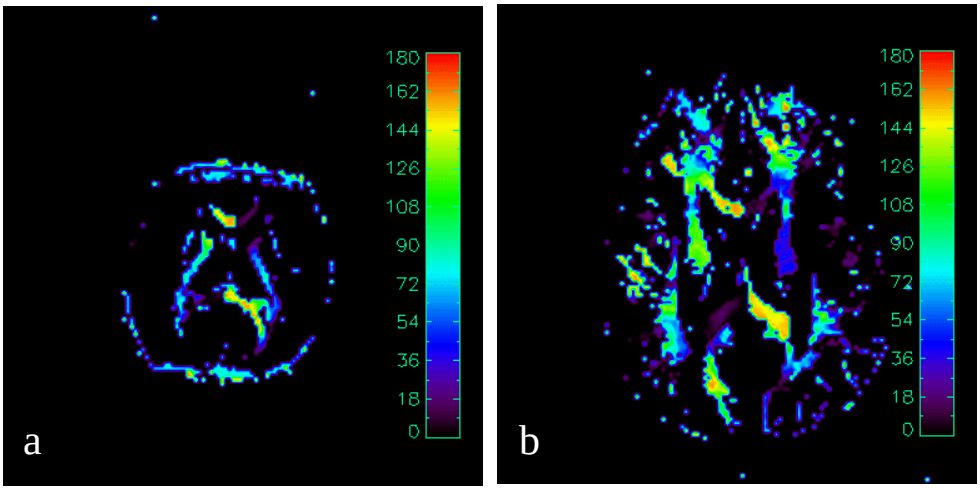

Fig. 5 Putative direction maps of the major white matter tracts are shown from one neonate and one adult, respectively. The color bars indicate the angles of the major white matter tracts in degrees with the zero degree corresponding to the positive x-axis.

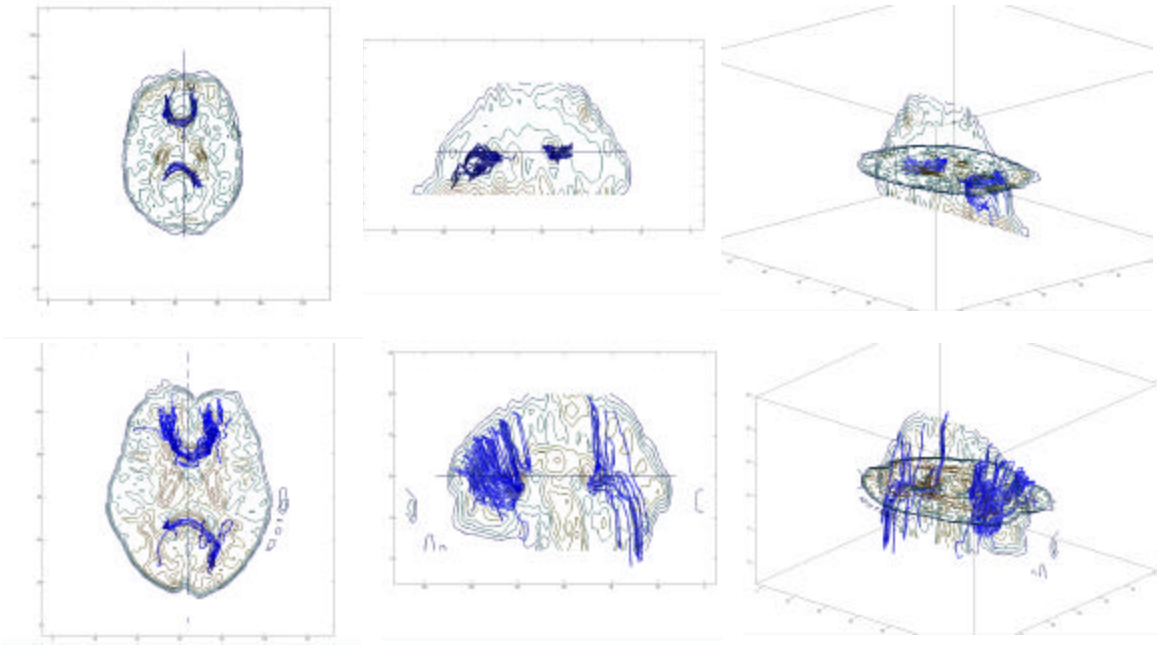

Fig. 6 Comparison of fiber tracking results obtained from a neonate (upper row) and an adult (lower row) subject. Fibers were tracked from the splenium and genu of the corpus callosum to the brain surface. The images illustrate top views (left), left views (middle) and top-oblique views (right). The resulting traces are overlaid with transversal and mid-sagittal contour plots of the DTI b=0 images.